ARTICLES

A luminal epithelial stem cell that is a cell of origin for prostate cancer

Xi Wang[1,2,5,6], Marianna Kruithof-de Julio[1,2], Kyriakos D. Economides[5,7]†, David Walker[5,6]†, Hailong Yu[5,6]†, M. Vivienne Halili[5,6]†, Ya-Ping Hu[5,6]†, Sandy M. Price[5,6], Cory Abate-Shen[3,4,5,7] & Michael M. Shen[1,2,5,6]

In epithelial tissues, the lineage relationship between normal progenitor cells and cell type(s) of origin for cancer has been poorly understood. Here we show that a known regulator of prostate epithelial differentiation, the homeobox gene *Nkx3-1*, marks a stem cell population that functions during prostate regeneration. Genetic lineage-marking demonstrates that rare luminal cells that express Nkx3-1 in the absence of testicular androgens (castration-resistant Nkx3-1-expressing cells, CARNs) are bipotential and can self-renew *in vivo*, and single-cell transplantation assays show that CARNs can reconstitute prostate ducts in renal grafts. Functional assays of *Nkx3-1* mutant mice in serial prostate regeneration suggest that *Nkx3-1* is required for stem cell maintenance. Furthermore, targeted deletion of the *Pten* tumour suppressor gene in CARNs results in rapid carcinoma formation after androgen-mediated regeneration. These observations indicate that CARNs represent a new luminal stem cell population that is an efficient target for oncogenic transformation in prostate cancer.

The prostate represents an excellent system for studying the function and molecular regulation of adult epithelial stem cells in the context of both tissue regeneration and cancer. The prostate epithelium is comprised of three differentiated cell types: luminal secretory cells, basal cells and neuroendocrine cells (Fig. 1a)[1]. Androgen-deprivation leads to rapid apoptosis of approximately 90% of luminal cells and a small percentage of basal cells, although a stable cell number is maintained in the regressed state[2,3]. After re-administration of androgens, the prostate epithelium regenerates over roughly 2 weeks[2–4], and is capable of more than 15 rounds of serial regression/regeneration[5,6], indicating that the prostate epithelium contains a long-term population of castration-resistant stem cells.

Substantial evidence supports the existence of a basal stem cell population in the prostate[7], consistent with analyses of progenitor cells in other epithelial tissues[8]. In particular, subpopulations of basal cells isolated using cell-surface markers show bipotentiality and self-renewal in explant culture and tissue grafts[9–13]. Furthermore, single Lin^- $Sca\text{-}1^+$ $CD133^+$ $CD44^+$ $CD117^+$ cells, which are predominantly basal in the mouse and exclusively basal in the human, can reconstitute prostatic ducts in renal grafts[14]. However, explants from *p63* (also known as *Trp63*)-null mice can form prostate tissue and undergo several rounds of serial regression/regeneration in the absence of basal cells[15], suggesting the existence of a distinct luminal stem cell population. Until now, however, luminal stem cells have not been identified in the prostate or other stratified epithelial tissues.

Although basal stem/progenitor cells have been proposed to represent a cell type of origin[7,16,17], human prostate cancer has a markedly luminal phenotype. Notably, the absence of basal cells is a diagnostic feature for prostate adenocarcinoma[18,19], suggesting either that prostate cancer arises from a luminal cell, or that oncogenic transformation of a basal progenitor results in rapid differentiation of luminal progeny. Here we show that expression of the *Nkx3-1* homeobox gene in the androgen-deprived prostate epithelium marks a rare luminal cell population that displays stem/progenitor properties during prostate regeneration. Our findings also indicate the relevance of this luminal stem cell population as a cell type of origin for prostate cancer.

Detection of CARNs in the prostate

The *Nkx3-1* homeobox gene regulates prostate epithelial differentiation, and is frequently inactivated at early stages of prostate tumorigenesis[20]. Notably, *Nkx3-1* homozygous mutant mice develop prostatic intraepithelial neoplasia (PIN), a precursor of prostate cancer, by 1 year of age[21–23]. In the intact adult mouse prostate, all luminal cells express *Nkx3-1*, and 9.5% of $p63^+$ basal cells ($n = 4{,}291$) also express *Nkx3-1* (Fig. 1b and Supplementary Fig. 1a)[24]. Previous studies have shown that *Nkx3-1* expression in prostate epithelial cells is reduced or abolished in the absence of androgens *in vivo*, and is consequently androgen-dependent[25,26]. Thus, Nkx3-1 expression is rapidly lost after castration, and Nkx3-1 expression is quickly restored after androgen re-administration to induce prostate regeneration (Fig. 1c, d and Supplementary Fig. 1b).

However, Nkx3-1 expression is not completely absent in the regressed prostate, but is instead retained in a rare population of epithelial cells (Fig. 1c, e). These castration-resistant Nkx3-1-expressing cells (CARNs) comprise 0.7% of total epithelial cells ($n = 38{,}329$) in the anterior prostate of androgen-deprived males, or approximately 460 CARNs per mouse (Supplementary Table 1, Methods). Furthermore, CARNs are frequently clustered (Fig. 1e), and can be detected in the ventral and dorsal prostate, as well as after a second round of regression (Supplementary Fig. 1c–f).

Notably, all CARNs in the regressed prostate are strictly luminal, because they never express the basal cell marker p63 ($n = 0$ out of 379) or the neuroendocrine marker synaptophysin ($n = 0$ out of 610) (Fig. 1f and Supplementary Table 1). Instead, CARNs express the

[1]Department of Medicine, [2]Department of Genetics and Development, [3]Department of Urology, and [4]Department of Pathology and Cell Biology, Herbert Irving Comprehensive Cancer Center, Columbia University College of Physicians and Surgeons, New York, New York 10032, USA. [5]Center for Advanced Biotechnology and Medicine, [6]Department of Pediatrics, and [7]Department of Medicine, UMDNJ–Robert Wood Johnson Medical School, Piscataway, New Jersey 08854, USA. †Present addresses: Department of Biological Sciences, Sanofi-Aventis, Bridgewater, New Jersey 08807, USA (K.D.E.); Department of Molecular Biology, Bristol-Myers Squibb Research Institute, Princeton, New Jersey 08543, USA (D.W.); Department of Food Science, Rutgers University, Piscataway, New Jersey 08901, USA (H.Y.); Cardiovascular Diseases Group, Merck Research Laboratories, Rahway, New Jersey 07065, USA (M.V.H.); Johnson and Johnson Skin Research Center, Skillman, New Jersey 08558, USA (Y.-P.H.); Department of Medical Oncology, Cancer Institute of New Jersey, New Brunswick, New Jersey 08903, USA (S.M.P.).

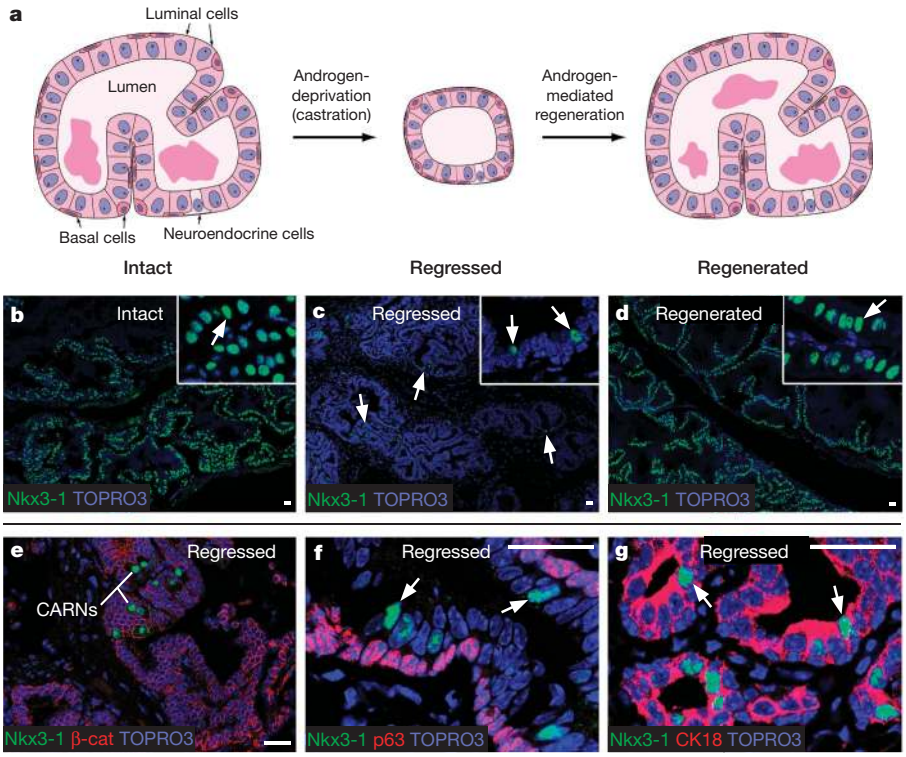

Figure 1 | Expression of *Nkx3-1* in epithelial cells of the intact, regressed and regenerated anterior prostate. **a**, Schematic prostate duct in the intact, regressed and regenerated states. Most luminal cells undergo apoptosis during regression, whereas most basal cells survive; hence, the process of regeneration primarily produces luminal cells. **b**, Nkx3-1 expression in all luminal cells of the wild-type intact prostate. **c**, Nkx3-1 expression is mostly absent in regressed prostate, except for rare castration-resistant Nkx3-1-expressing cells (CARNs, arrows). **d**, Expression of Nkx3-1 in regenerated prostate, showing similarity to **b**. **e**, Immunostaining for Nkx3-1 and β-catenin shows clustering of CARNs. **f**, **g**, CARNs are strictly luminal, as shown by the lack of co-staining for Nkx3-1 (arrows) and p63 (**f**), and by co-localization of Nkx3-1 (arrows) with CK18 (**g**). Scale bars, 25 μm.

luminal markers cytokeratin 18 (CK18, also known as Krt18) ($n = 828$ out of 837) and androgen receptor ($n = 46$ out of 46), and are growth-quiescent, as they do not co-express Ki67 (also known as Mki67; $n = 0$ out of 151) (Fig. 1g and Supplementary Fig. 1g, h). The CARN population is non-overlapping with the Lin^- $Sca\text{-}1^+$ $CD133^+$ $CD44^+$ $CD117^+$ stem/progenitor population[14], because CD117 (also known as Kit)-positive cells in regressed prostate are never luminal ($n = 0$ out of 79) (Supplementary Fig. 1k, l). Furthermore, because the CARN population is strictly luminal, it is also distinct from other previously described prostate stem cell populations that are exclusively basal[9,10,13].

Bipotentiality and self-renewal

To investigate whether the CARN population might correspond to prostate epithelial progenitors, we performed *in vivo* lineage-marking using a knock-in allele that places a tamoxifen-inducible Cre recombinase[27,28] under the transcriptional control of the *Nkx3-1* promoter (Supplementary Fig. 2a). We assessed the specificity of this tamoxifen-inducible *Nkx3-1*^{CreERT2} allele in control crosses with the *R26R-YFP* Cre-reporter[29] and the *R26R-lacZ* alleles[30], and found that Cre-mediated recombination after tamoxifen administration closely recapitulates the endogenous pattern of *Nkx3-1* expression in the intact prostate (Supplementary Fig. 2b–f).

We performed lineage-marking of CARNs by tamoxifen treatment of castrated *Nkx3-1*$^{CreERT2/+}$*; R26R-YFP/+* or *Nkx3-1*$^{CreERT2/+}$*; R26R-lacZ/+* adult males (Fig. 2a, b). As expected for genetic marking of CARNs in regressed prostate, we observed yellow fluorescent protein (YFP) or β-galactosidase expression in rare epithelial cells that were strictly luminal (Supplementary Table 1). These lineage-marked cells were never positive for the basal markers p63 ($n = 0$ out of 98) or CK14 (also known as Krt14; $n = 0$ out of 131), and almost never positive for CK5 (Krt5; $n = 2$ out of 93), but always expressed the luminal markers CK18 ($n = 123$ out of 123) and androgen receptor ($n = 94$ out of 94) (Fig. 2c and Supplementary Fig. 3a–d). After regeneration, the percentage of lineage-marked cells increased ninefold (from 0.37% ($n = 19{,}825$) to 3.3% ($n = 95{,}017$), $P < 0.0001$) (Fig. 2d), indicating the proliferative potential of CARNs. Although most of the lineage-marked cells in regenerated prostates were luminal, we observed occasional YFP^+ $CK5^+$, YFP^+ $p63^+$, or β-gal^+ $CK14^+$ basal cells, corresponding to 3.0% of lineage-marked cells ($n = 559$) (Fig. 2e and Supplementary Fig. 3g–l); this percentage of regenerated basal cells is consistent with the low percentage of basal cells lost during regression[2]. Because all of the lineage-marked cells were luminal in the regressed prostate, but could give rise to both basal and luminal cells during regeneration, we conclude that the initial CARN population contains bipotential progenitors.

To investigate the self-renewal of CARNs, we examined whether they could undergo at least one cell division during prostate regeneration to generate a daughter cell that is also a CARN. We determined whether lineage-marked CARNs in castrated *Nkx3-1*$^{CreERT2/+}$*; R26R-YFP/+* mice would incorporate BrdU during prostate regeneration, while retaining CARN identity (Nkx3-1 expression) after a subsequent prostate regression (Fig. 2f and Supplementary Fig. 3m). Such triple-positive $Nkx3\text{-}1^+$ YFP^+ $BrdU^+$ cells were observed (Fig. 2g–i), providing evidence for CARN self-renewal. In particular, the percentage of $BrdU^+$ cells among $Nkx3\text{-}1^+$ YFP^+ cells, corresponding to CARNs in both the first and second regression, represents the percentage of CARNs undergoing a self-renewal division (24%, $n = 68$; Supplementary Table 2).

To assess long-term self-renewal, we examined the persistence of lineage-marked cells in *Nkx3-1*$^{CreERT2/+}$*; R26R-YFP/+* mice after four rounds of regression/regeneration (Fig. 2j). In these mice, YFP^+ cells represented 3.0% ($n = 21{,}559$) of the prostate epithelium, similar to the percentage observed after one round (Fig. 2k, l). The persistence of YFP^+ cells is consistent with the maintenance of a constant stem cell number during regeneration, as suggested by the

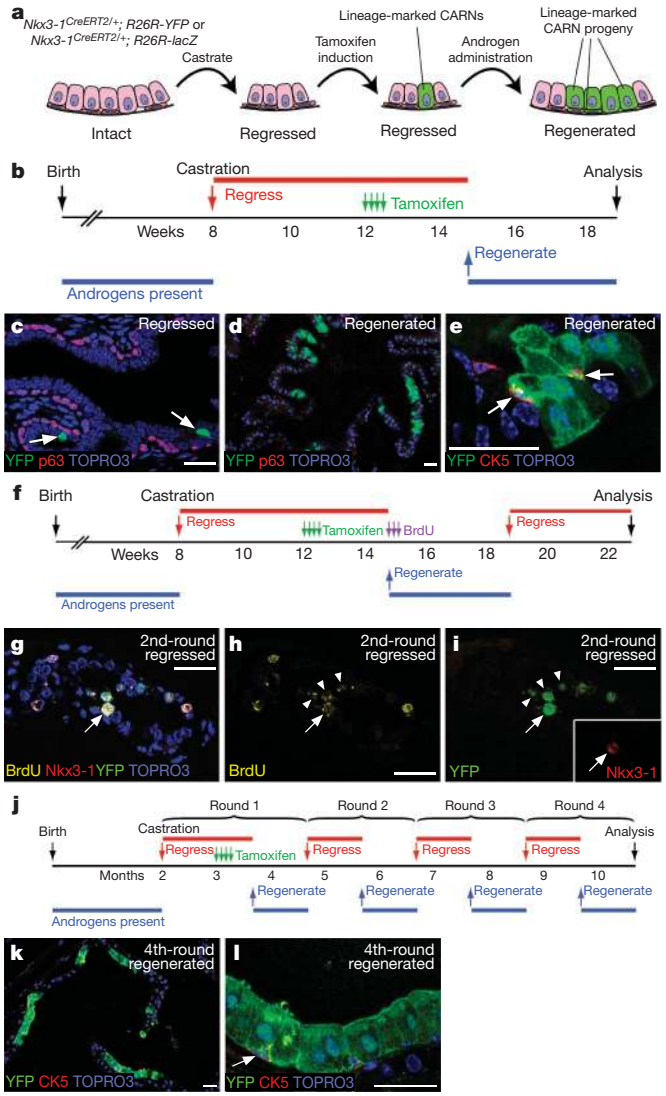

Figure 2 | Bipotentiality and self-renewal of CARNs *in vivo*. **a**, Strategy for lineage-marking experiment. **b**, Time-line for the experiment. **c**, YFP does not co-localize with p63 in lineage-marked cells of a castrated and tamoxifen-induced *Nkx3-1*$^{CreERT2/+}$*; R26R-YFP/+* anterior prostate. **d**, Clusters of YFP$^+$ cells in a lineage-marked and regenerated prostate. **e**, Co-localization of YFP and CK5 in lineage-marked basal cells (arrows) of a regenerated prostate. **f**, Time-line for self-renewal experiment. **g–i**, Co-localization of Nkx3-1, YFP and BrdU immunostaining (arrow) in anterior prostate, shown as an overlay (**g**) and individual channels (**h**, **i**); YFP$^+$ BrdU$^+$ neighbours are indicated (arrowheads). **j**, Strategy for four-round serial regression/regeneration assay of long-term CARN self-renewal. **k**, **l**, Clusters of YFP$^+$ cells in the lineage-marked prostate after four rounds of serial regression/regeneration. Scale bars, 25 μm.

ability of the epithelium to undergo apparently unlimited serial regeneration[5,6], and supports the long-term self-renewal of lineage-marked CARNs.

Single-cell transplantation of CARNs

Next, we investigated whether CARNs could reconstitute prostate tissue in grafts generated from single or multiple lineage-marked CARNs (Fig. 3a and Supplementary Fig. 4). To examine single lineage-marked CARNs, we isolated individual YFP$^+$ cells from suspensions of dissociated prostate cells, followed by recombination with rat urogenital mesenchyme cells and renal grafting in immunodeficient male mice (Supplementary Fig. 5a–f). The resulting grafts generated prostatic ducts with epithelial cells that were entirely YFP$^+$ and that expressed luminal markers (E-cadherin, CK18 and androgen receptor), basal markers (p63 and CK5), or neuroendocrine markers (synaptophysin) (Fig. 3b–h and Supplementary Fig. 5g, h); in particular, these ducts produced secretory proteins and expressed Nkx3-1, which is prostate-specific (Fig. 3c, i). Furthermore, we verified that the tissue formed in these grafts was unequivocally of mouse origin by nuclear morphology[31] (Supplementary Fig. 6). Notably, the frequency of successful single-cell transplantation of lineage-marked YFP$^+$ cells (37%, $n = 43$) was significantly greater than for the YFP$^-$ control (3%, $n = 31$; $P < 0.001$) (Fig. 3j).

Nkx3-1 regulates progenitor maintenance

Because *Nkx3-1* expression marks the CARN population, we next investigated whether *Nkx3-1* regulates progenitor maintenance and/or differentiation. First, we examined whether BrdU label-retaining cells (LRCs) might be affected by *Nkx3-1* inactivation, because in many tissues (but not all[32]) such long-term growth-quiescent cells are enriched for progenitors[33,34]. In the prostate, such LRCs can be identified by BrdU pulse-chase labelling during serial regression/regeneration[6] (Fig. 4a). Under conditions in which 1.4% of epithelial cells ($n = 33{,}086$) retained BrdU-labelling at the fifth regression, 14.0% of CARNs ($n = 193$) were also BrdU-positive (Fig. 4b–d and Supplementary Table 3), indicating that a significant proportion of CARNs are also LRCs. Second, the percentage of LRCs in *Nkx3-1* mutants (0.3%, $n = 86{,}601$) was significantly less than in wild-type controls (0.8%, $n = 75{,}758$; $P = 0.003$) after five rounds of regression/regeneration (Fig. 4e–g and Supplementary Table 3), suggesting a decrease in prostate epithelial progenitors.

We also observed phenotypic alterations in *Nkx3-1* mutants after five rounds of serial regeneration, including reduced anterior prostate volume relative to wild-type controls (Fig. 4h). At the histological level, the characteristic hyperplasia and PIN phenotype of *Nkx3-1* homozygous ($n = 10$) as well as heterozygous ($n = 8$) mice was partially suppressed by five rounds of serial regeneration, whereas no abnormalities were observed in wild-type controls ($n = 9$) treated in parallel; similar results were observed after three rounds of serial regeneration (Supplementary Figs 7, 8 and Supplementary Table 4). Notably, the proliferative index of serially regenerated *Nkx3-1*$^{-/-}$ mutants was similar to controls (Supplementary Fig. 8h, i), in contrast with the increased proliferation observed in intact *Nkx3-1* homozygotes[21]. Overall, these findings suggest that *Nkx3-1* is required for prostate stem cell maintenance during serial regression/regeneration.

CARNs are a cell of origin for cancer

We also investigated whether CARNs could represent a target of oncogenic transformation in prostate cancer, by examining the effects of CARN-specific deletion of the tumour suppressor gene *Pten*, an important regulator of the PI3-kinase/Akt signalling pathway that is frequently inactivated in human prostate cancer. For this purpose, we inducibly deleted *Pten* in the CARN population of castrated male mice carrying a conditional *Pten* allele[35] together with the inducible *Nkx3-1*^{CreERT2} allele (Fig. 5a). After androgen-mediated regeneration of the prostate, we observed rapid formation of high-grade PIN and carcinoma with evidence of microinvasion in the *Nkx3-1*$^{CreERT2/+}$*; Pten*$^{flox/flox}$ mice ($n = 6$), whereas control *Nkx3-1*$^{CreERT2/+}$*; Pten*$^{+/+}$ mice were phenotypically normal ($n = 6$) (Fig. 5b–e). Notably, these PIN and carcinoma lesions showed increased proliferation and loss of basal cells, and displayed membrane-localized phosphorylated-Akt activity (Fig. 5f–m). These data indicate that the CARN population can act as a cell of origin for prostate cancer, and that the resulting carcinoma lesions have a luminal phenotype.

Discussion

Together with previous studies describing basal stem cells[9,10,13], our identification of CARNs as luminal stem cells indicates the existence of distinct non-overlapping stem cell populations in the prostate epithelium. Consequently, we can propose two general models for

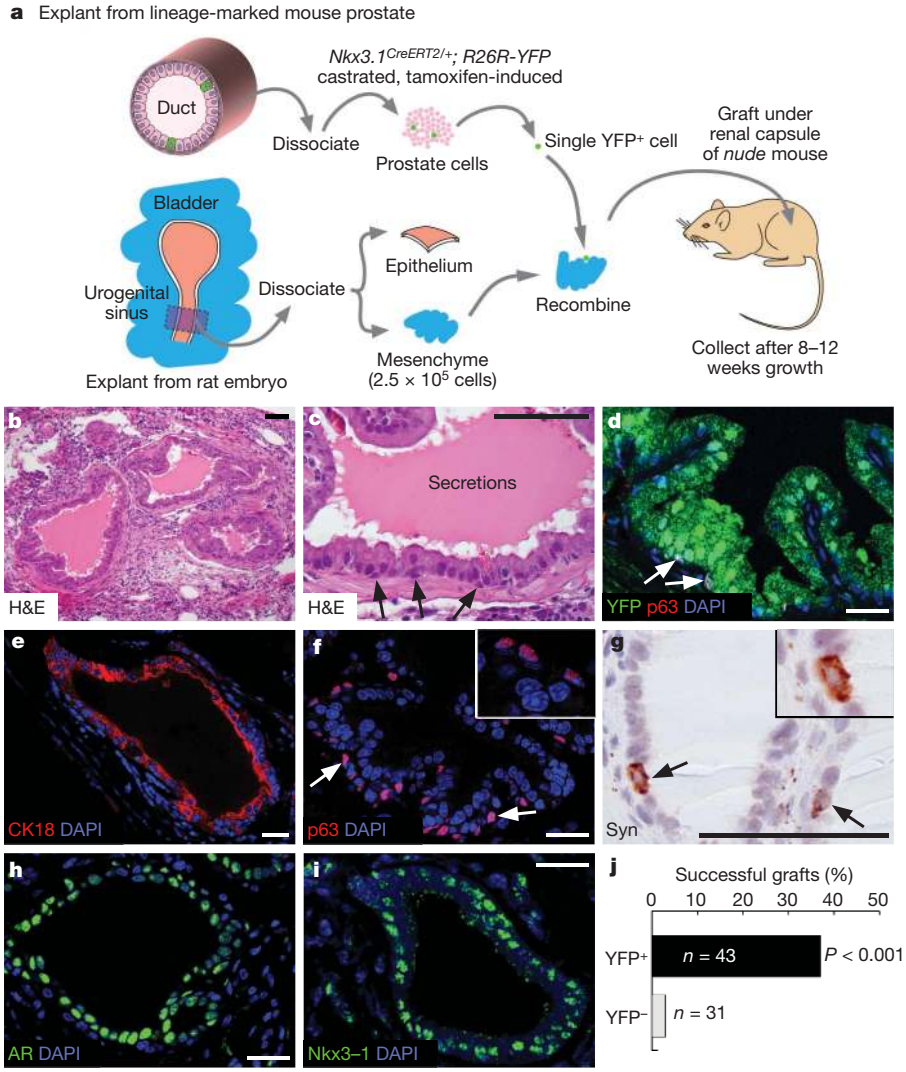

Figure 3 | Generation of prostatic ducts in renal grafts by single lineage-marked CARNs. **a**, Strategy for tissue recombinant/renal graft analyses using a single YFP$^+$ cell (or single YFP$^-$ cell as a control). **b**, **c**, Haematoxylin and eosin (H&E) staining of prostatic ducts in a graft derived from a single YFP$^+$ cell; note the presence of basal cells (arrows) and secretions (**c**). **d**, All epithelial cells in single-YFP$^+$-derived duct express YFP, including p63$^+$ basal cells (arrows). **e**–**g**, Expression of luminal marker CK18 (**e**), basal marker p63 (**f**), and neuroendocrine marker synaptophysin (Syn) (**g**) in ducts from single YFP$^+$ cells. **h**, **i**, Expression of androgen receptor (AR) (**h**) and Nkx3-1 (**i**) confirm prostate identity of ducts. **j**, Summary of single-cell transplantation data. Scale bars, 25 μm (**d**–**f**, **h**, **i**) and 50 μm (**b**, **c**, **g**).

the lineage relationship between CARNs and a basal stem cell population. One possibility is that basal and luminal cell types may possess independent progenitors that have partially redundant stem cell activities (Fig. 6a). A second possibility is that CARNs represent facultative or 'potential' stem cells corresponding to transit-amplifying cells that acquire stem cell properties during regeneration/wound healing responses, as has been described in the mammalian testis and pancreas[36–38] (Fig. 6b). In this model, the facultative stem cells that drive prostate regeneration could be independent from the stem cells for prostate organogenesis, and might co-exist in the adult gland; such a dual progenitor system functions during *Drosophila* tracheal remodelling[39].

Furthermore, the observed defect in stem cell maintenance in *Nkx3-1* mutants suggests a functional role for *Nkx3-1* expression in CARNs.

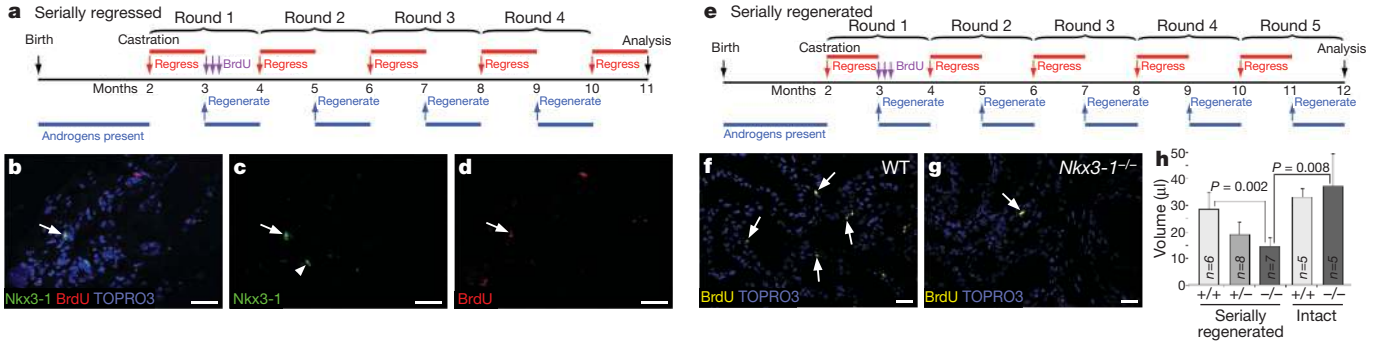

Figure 4 | *Nkx3-1* mutants display prostate epithelial defects in a serial regeneration assay. **a**, Time-line for analysis of LRCs. **b**–**d**, Overlap of CARNs with LRCs in a serially regressed prostate, shown as an overlay (**b**) and individual panels (**c**, **d**). Arrows in **b**–**d** indicate a Nkx3-1$^+$ BrdU$^+$ cell; arrowhead in **c** indicates a CARN that is BrdU$^-$. **e**, Time-line for serial regression/regeneration analyses. **f**, **g**, Decreased number of LRCs (arrows) in *Nkx3-1*$^{-/-}$ anterior prostate (**g**) relative to wild-type (WT) controls (**f**) after serial regeneration. **h**, Decreased volume of *Nkx3-1*$^{-/-}$ anterior prostate relative to wild-type and *Nkx3-1*$^{+/-}$ prostates after serial regeneration, and to intact wild-type and *Nkx3-1*$^{-/-}$ prostates. Error bars correspond to one standard deviation. Scale bars, 25 μm.

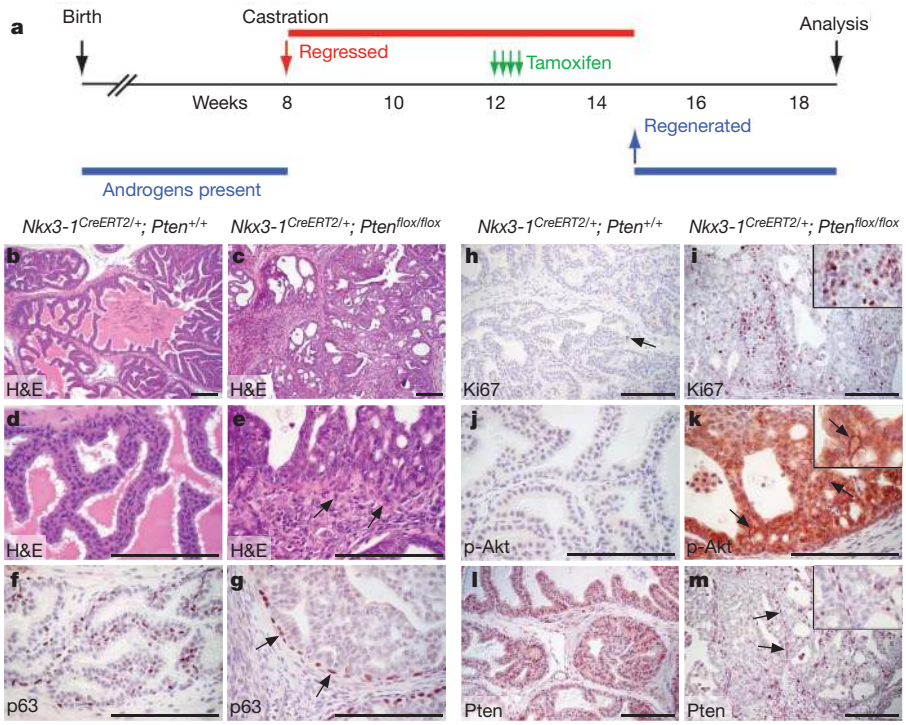

Figure 5 | The CARN population contains a cell type of origin for prostate cancer. **a**, Time-line for inducible conditional deletion of *Pten* in CARNs. **b**–**e**, H&E staining of anterior prostate from control *Nkx3-1*$^{CreERT2/+}$; *Pten*$^{+/+}$ (**b**, **d**) and *Nkx3-1*$^{CreERT2/+}$; *Pten*$^{flox/flox}$ (**c**, **e**) mice, shown at low-power (**b**, **c**) and high-power (**d**, **e**). The *Nkx3-1*$^{CreERT2/+}$; *Pten*$^{flox/flox}$ prostate contains high-grade PIN/carcinoma lesions with local invasive epithelium (arrows, **e**). **f**, **g**, Detection of p63^{+} basal cells shows loss of basal cells except at the periphery (arrows, **g**) of PIN/carcinoma lesions. **h**, **i**, Increased Ki67 immunostaining in PIN/carcinoma lesions. **j**, **k**, Phosphorylated-Akt (p-Akt) immunostaining with cell membrane localization (arrows, **k**) in PIN/carcinoma lesions. **l**, **m**, Pten immunostaining is ubiquitous in control *Nkx3-1*$^{CreERT2/+}$; *Pten*$^{+/+}$ prostate epithelium, but is restricted to basal cells (arrows) and scattered luminal cells in induced *Nkx3-1*$^{CreERT2/+}$; *Pten*$^{flox/flox}$ prostate. Scale bars, 100 μm.

Thus, *Nkx3-1* inactivation might result in increased differentiation of CARNs and expansion of a proliferative transit-amplifying population (Supplementary Fig. 9). This interpretation is consistent with the finding that the duration of epithelial proliferation during prostate regeneration is prolonged in *Nkx3-1* mutants relative to wild type[40]. The function of *Nkx3-1* in stem-cell maintenance may be direct, consistent with its feedback loop with the androgen receptor and its role in prostate epithelial differentiation[20,41], or may be indirect, for example owing to increased oxidative damage with ageing[42].

Finally, the importance of the stem cell compartment as a target of oncogenic transformation has been highlighted by studies showing that stem cell populations in the lung and colon are efficient cells of origin for cancer[43,44]. In the case of prostate cancer, the identification of a castration-resistant stem cell population as a cell of origin also has implications for the onset of hormone-refractory disease. Thus, if oncogenic transformation of CARNs can result in the formation of a putative cancer stem cell, the eventual emergence of hormone-refractory disease may be prefigured through an initiating event during prostate carcinogenesis.

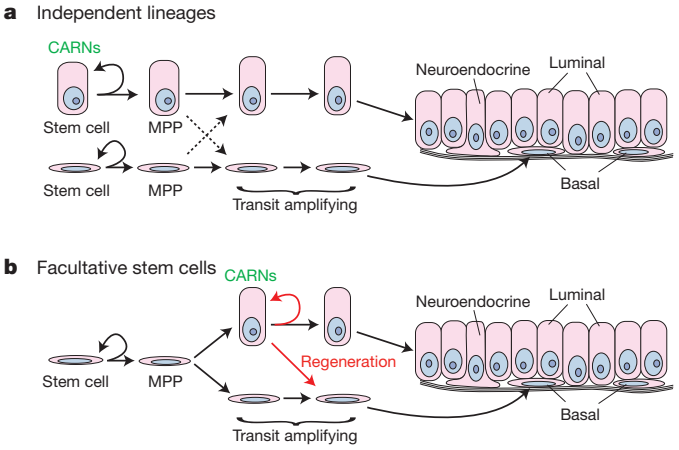

Figure 6 | Possible lineage relationships in the prostate epithelium. **a**, Independent stem cells for basal and luminal epithelium may give rise to differentiated cell types through multipotent progenitors (MPP) and transit-amplifying progenitors, with some bipotentiality (dashed arrows). In this model, CARNs would correspond to the luminal stem cells. **b**, Alternatively, stem cells for prostate organogenesis may be basal, but luminal transit-amplifying cells, including CARNs, can acquire stem cell properties during regeneration (red arrows), thus acting as facultative or potential stem cells.

METHODS SUMMARY

The *Nkx3-1*$^{CreERT2/+}$ allele was generated by gene targeting using standard techniques; the *Nkx3-1*-null mutant mice have been previously described[21]. *R26R-lacZ* and *Pten* conditional mutant mice were obtained from the Jackson Laboratory Induced Mutant Resource; the *R26R-YFP* mice were provided by F. Costantini. All lines were maintained on a hybrid C57BL/6-129/Sv strain background.

Castration of adult male mice was performed using standard techniques. For tamoxifen induction of Cre activity in mice containing *Nkx3-1*$^{CreERT2/+}$, mice were administered 9 mg per 40 g tamoxifen for 4 consecutive days. For prostate regeneration, physiological levels of testosterone (1.875 μg h^{-1}) were administered for 4 weeks by subcutaneous implantation of mini-osmotic pumps (Alzet)[45]. When included, BrdU (100 mg kg^{-1}) was administered once daily during the first 3 days of regeneration. For single-cell transplantation, single YFP^{+} cells were isolated by mouth-pipetting under epifluorescence illumination from a dissociated prostate cell suspension obtained from castrated and tamoxifen-induced *Nkx3-1*$^{CreERT2/+}$; *R26R-YFP*/+ mice. A single YFP^{+} cell (or YFP^{-} cell as a control) was recombined with 2.5×10^{5} rat urogenital sinus mesenchyme cells in a 10-μl collagen pad, followed by transplantation under the kidney capsule of *nude* mice and collecting after 10–12 weeks.

Cryosections were stained with primary antibodies as listed in Supplementary Table 5, and counterstained with TOPRO3 or 4,6-diamidino-2-phenylindole

(DAPI) (Invitrogen/Molecular Probes). Secondary antibodies were labelled with Alexa Fluor 488, 555 or 594 (Invitrogen/Molecular Probes). Immunofluorescence staining was imaged using a Leica TCS5 spectral confocal microscope. Cell counting was performed manually using confocal photomicrographs with at least three animals for each experiment or genotype analysed.

Full Methods and any associated references are available in the online version of the paper at www.nature.com/nature.

Received 11 April 2008; accepted 5 August 2009.
Published online 9 September 2009.

1. Abate-Shen, C. & Shen, M. M. Molecular genetics of prostate cancer. *Genes Dev.* **14,** 2410–2434 (2000).
2. English, H. F., Santen, R. J. & Isaacs, J. T. Response of glandular versus basal rat ventral prostatic epithelial cells to androgen withdrawal and replacement. *Prostate* **11,** 229–242 (1987).
3. Evans, G. S. & Chandler, J. A. Cell proliferation studies in the rat prostate: II. The effects of castration and androgen-induced regeneration upon basal and secretory cell proliferation. *Prostate* **11,** 339–351 (1987).
4. Sugimura, Y., Cunha, G. R. & Donjacour, A. A. Morphological and histological study of castration-induced degeneration and androgen-induced regeneration in the mouse prostate. *Biol. Reprod.* **34,** 973–983 (1986).
5. Isaacs, J. T. in *Benign Prostatic Hyperplasia* (eds Rodgers C. H. *et al.*) 85–94 (Department of Health and Human Services, 1985).
6. Tsujimura, A. *et al.* Proximal location of mouse prostate epithelial stem cells: a model of prostatic homeostasis. *J. Cell Biol.* **157,** 1257–1265 (2002).
7. Lawson, D. A. & Witte, O. N. Stem cells in prostate cancer initiation and progression. *J. Clin. Invest.* **117,** 2044–2050 (2007).
8. Senoo, M., Pinto, F., Crum, C. P. & McKeon, F. p63 is essential for the proliferative potential of stem cells in stratified epithelia. *Cell* **129,** 523–536 (2007).
9. Lawson, D. A., Xin, L., Lukacs, R. U., Cheng, D. & Witte, O. N. Isolation and functional characterization of murine prostate stem cells. *Proc. Natl Acad. Sci. USA* **104,** 181–186 (2007).
10. Richardson, G. D. *et al.* CD133, a novel marker for human prostatic epithelial stem cells. *J. Cell Sci.* **117,** 3539–3545 (2004).
11. Burger, P. E. *et al.* Sca-1 expression identifies stem cells in the proximal region of prostatic ducts with high capacity to reconstitute prostatic tissue. *Proc. Natl Acad. Sci. USA* **102,** 7180–7185 (2005).
12. Xin, L., Lawson, D. A. & Witte, O. N. The Sca-1 cell surface marker enriches for a prostate-regenerating cell subpopulation that can initiate prostate tumorigenesis. *Proc. Natl Acad. Sci. USA* **102,** 6942–6947 (2005).
13. Goldstein, A. S. *et al.* Trop2 identifies a subpopulation of murine and human prostate basal cells with stem cell characteristics. *Proc. Natl Acad. Sci. USA* **105,** 20882–20887 (2008).
14. Leong, K. G., Wang, B. E., Johnson, L. & Gao, W. Q. Generation of a prostate from a single adult stem cell. *Nature* **456,** 804–808 (2008).
15. Kurita, T., Medina, R. T., Mills, A. A. & Cunha, G. R. Role of p63 and basal cells in the prostate. *Development* **131,** 4955–4964 (2004).
16. Kasper, S. Stem cells: the root of prostate cancer? *J. Cell. Physiol.* **216,** 332–336 (2008).
17. Wang, S. *et al.* Pten deletion leads to the expansion of a prostatic stem/progenitor cell subpopulation and tumor initiation. *Proc. Natl Acad. Sci. USA* **103,** 1480–1485 (2006).
18. Grisanzio, C. & Signoretti, S. p63 in prostate biology and pathology. *J. Cell. Biochem.* **103,** 1354–1368 (2008).
19. Humphrey, P. A. Diagnosis of adenocarcinoma in prostate needle biopsy tissue. *J. Clin. Pathol.* **60,** 35–42 (2007).
20. Abate-Shen, C., Shen, M. M. & Gelmann, E. Integrating differentiation and cancer: the *Nkx3.1* homeobox gene in prostate organogenesis and carcinogenesis. *Differentiation* **76,** 717–727 (2008).
21. Bhatia-Gaur, R. *et al.* Roles for *Nkx3.1* in prostate development and cancer. *Genes Dev.* **13,** 966–977 (1999).
22. Abdulkadir, S. A. *et al.* Conditional loss of *Nkx3.1* in adult mice induces prostatic intraepithelial neoplasia. *Mol. Cell. Biol.* **22,** 1495–1503 (2002).
23. Kim, M. J. *et al. Nkx3.1* mutant mice recapitulate early stages of prostate carcinogenesis. *Cancer Res.* **62,** 2999–3004 (2002).
24. Chen, H., Mutton, L. N., Prins, G. S. & Bieberich, C. J. Distinct regulatory elements mediate the dynamic expression pattern of *Nkx3.1. Dev. Dyn.* **234,** 961–973 (2005).
25. Sciavolino, P. J. *et al.* Tissue-specific expression of murine *Nkx3.1* in the male urogenital system. *Dev. Dyn.* **209,** 127–138 (1997).
26. Bieberich, C. J., Fujita, K., He, W.-W. & Jay, G. Prostate-specific and androgen-dependent expression of a novel homeobox gene. *J. Biol. Chem.* **271,** 31779–31782 (1996).
27. Feil, R., Wagner, J., Metzger, D. & Chambon, P. Regulation of Cre recombinase activity by mutated estrogen receptor ligand-binding domains. *Biochem. Biophys. Res. Commun.* **237,** 752–757 (1997).
28. Indra, A. K. *et al.* Temporally-controlled site-specific mutagenesis in the basal layer of the epidermis: comparison of the recombinase activity of the tamoxifen-inducible Cre-ER(T) and Cre-ER(T2) recombinases. *Nucleic Acids Res.* **27,** 4324–4327 (1999).
29. Srinivas, S. *et al.* Cre reporter strains produced by targeted insertion of *EYFP* and *ECFP* into the *ROSA26* locus. *BMC Dev. Biol.* **1,** 4 (2001).
30. Soriano, P. Generalized *lacZ* expression with the ROSA26 Cre reporter strain. *Nature Genet.* **21,** 70–71 (1999).
31. Cunha, G. R. & Vanderslice, K. D. Identification in histological sections of species origin of cells from mouse, rat and human. *Stain Technol.* **59,** 7–12 (1984).
32. Kiel, M. J. *et al.* Haematopoietic stem cells do not asymmetrically segregate chromosomes or retain BrdU. *Nature* **449,** 238–242 (2007).
33. Bickenbach, J. R. & Holbrook, K. A. Label-retaining cells in human embryonic and fetal epidermis. *J. Invest. Dermatol.* **88,** 42–46 (1987).
34. Cotsarelis, G., Cheng, S. Z., Dong, G., Sun, T. T. & Lavker, R. M. Existence of slow-cycling limbal epithelial basal cells that can be preferentially stimulated to proliferate: implications on epithelial stem cells. *Cell* **57,** 201–209 (1989).
35. Groszer, M. *et al.* Negative regulation of neural stem/progenitor cell proliferation by the Pten tumor suppressor gene *in vivo. Science* **294,** 2186–2189 (2001).
36. Nakagawa, T., Nabeshima, Y. & Yoshida, S. Functional identification of the actual and potential stem cell compartments in mouse spermatogenesis. *Dev. Cell* **12,** 195–206 (2007).
37. Xu, X. *et al.* Beta cells can be generated from endogenous progenitors in injured adult mouse pancreas. *Cell* **132,** 197–207 (2008).
38. Barroca, V. *et al.* Mouse differentiating spermatogonia can generate germinal stem cells *in vivo. Nature Cell Biol.* **11,** 190–196 (2009).
39. Weaver, M. & Krasnow, M. A. Dual origin of tissue-specific progenitor cells in *Drosophila* tracheal remodeling. *Science* **321,** 1496–1499 (2008).
40. Magee, J. A., Abdulkadir, S. A. & Milbrandt, J. Haploinsufficiency at the *Nkx3.1* locus: a paradigm for stochastic, dosage-sensitive gene regulation during tumor initiation. *Cancer Cell* **3,** 273–283 (2003).
41. Lei, Q. *et al.* NKX3.1 stabilizes p53, inhibits AKT activation, and blocks prostate cancer initiation caused by PTEN loss. *Cancer Cell* **9,** 367–378 (2006).
42. Ouyang, X., DeWeese, T. L., Nelson, W. G. & Abate-Shen, C. Loss-of-function of *Nkx3.1* promotes increased oxidative damage in prostate carcinogenesis. *Cancer Res.* **65,** 6773–6779 (2005).
43. Kim, C. F. *et al.* Identification of bronchioalveolar stem cells in normal lung and lung cancer. *Cell* **121,** 823–835 (2005).
44. Barker, N. *et al.* Crypt stem cells as the cells-of-origin of intestinal cancer. *Nature* **457,** 608–611 (2009).
45. Banach-Petrosky, W. *et al.* Prolonged exposure to reduced levels of androgen accelerates prostate cancer progression in *Nkx3.1; Pten* mutant mice. *Cancer Res.* **67,** 9089–9096 (2007).

Supplementary Information is linked to the online version of the paper at www.nature.com/nature.

Acknowledgements We thank M. Kim for her initial observations on *Nkx3-1* expression in the regressed prostate, and C. Cordon-Cardo, E. Gelmann, C. Mendelsohn and B. Reizis for comments on the manuscript. We are also grateful to C. Bieberich, M. Capecchi, P. Chambon and F. Costantini for providing mice and reagents. This work was supported by grants from the NIH (C.A.-S. and M.M.S.), DOD Prostate Cancer Research Program (K.D.E., C.A.-S. and M.M.S.), and the NCI Mouse Models of Human Cancer Consortium.

Author Contributions X.W., M.K.-D., K.D.E., C.A.-S. and M.M.S. designed experiments, Y.P.-H. and S.M.P. generated mouse reagents, X.W., M.K.-D., K.D.E., D.W., H.Y. and M.V.H. performed experiments, and X.W., M.K.-D., C.A.-S. and M.M.S. wrote the manuscript.

Author Information Reprints and permissions information is available at www.nature.com/reprints. Correspondence and requests for materials should be addressed to M.M.S. (mshen@columbia.edu).

METHODS

Gene targeting and genotyping. The *Nkx3-1*$^{CreERT2/+}$ allele was generated by gene targeting using standard techniques[46]. The targeting vector was generated using a 5′ arm corresponding to a 3.5-kilobase (kb) PCR fragment from a *Nkx3-1* genomic clone[21] up to the translation initiation site of Nkx3-1, and a 3′ arm corresponding to a 4.0-kb PCR fragment of genomic sequence (Supplementary Fig. 2a). The positive-selection cassette corresponded to the self-excising ACE-Cre/PolII-neo selection cassette from the pACN vector[47], whereas negative selection was provided by the PGK-tk cassette from the pPNT vector[48]. Primers for generating the 5′ arm were 5′-ACCGGAATTCTCCGCTGCGCGCCGCTTTTGC-3′ and 5′-ACCCAAGCTTCATGCCTGCAGGTCGGAGGCC-3′. Primers to amplify the 3′ arm were 5′-CTAGTCTAGAGCGGCTCACCTCCTTCCTCA-3′ and 5′-CTAGTCTAGAGGATGGCAGGAGAGGTCACTGC-3′. The gap between the 5′ and 3′ arms is approximately 80 base pairs (bp), such that the 3′ arm contains most of exon 1 together with intron 1, exon 2 and 200 bp of genomic sequence 3′ of the transcription termination site. The pGS-CreER^{T2} vector[28] was provided by P. Chambon, and was modified by the insertion of a 65-bp intron from ACE-Cre[47] between the PshAI and ClaI sites of the CreER^{T2} sequence. Culture and transfection of mouse embryonic stem (ES) cells followed standard protocols[46]. Homologous recombinants in TC1 ES cells[49] were selected by positive-negative selection followed by Southern blot screening. One out of two-hundred-and-sixty clones analysed was properly targeted, and this clone was used to generate germline chimaeras.

Mouse genotyping. Genotyping for the *Nkx3-1*^{CreRT2} allele was performed by Southern blotting or by PCR using tail genomic DNA. Primers for PCR genotyping were as follows: for the *Nkx3-1* wild-type allele, 5′-CTCCGCTACCCTAAGCATCC-3′ and 5′-GACACTGTCATATTACTTGGACC-3′, which amplifies a region deleted in the targeting vector; and for the *Nkx3-1*^{CreERT2} allele, 5′-CAGATGGCGCGGCAACACC-3′ and 5′-GCGCGGTCTGGCAGTAAAAAC-3′.

The primers for genotyping *Nkx3-1* mutant mice were 5′-GCCAACCTGCCTCAATCACTAAGG-3′ (wild-type *Nkx3-1* forward), 5′-TTCCACATACACTTCATTCTCAGT-3′ (mutated forward), and 5′-GCCAACCTGCCTCAATCACTAAGG-3′ (wild-type and mutated reverse). The primers for genotyping the *R26R-lacZ* Cre-reporter were 5′-CCGCGCTGTACTGGAGGCTGAAG-3′ (forward) and 5′-ATACTGCACCGGGCGGGAAGGAT-3′ (reverse). Primers for genotyping the *Pten* conditional (*Pten*^{flox}) allele were 5′-ACTCAAGGCAGGGATGAGC-3′ (forward) and 5′-GTCATCTTCACTTAGCCATTGG-3′ (reverse). Primers for genotyping the *R26R-YFP* mice were 5′-GCGAAGAGTTTGTCCTCAACC-3′ (mutated forward), 5′-GGAGCGGGAGAAATGGATATG-3′ (wild-type forward) and 5′-AAAGTCGCTCTGAGTTGTTAT-3′ (wild-type and mutated reverse).

Mouse procedures. Castration of adult male mice was performed using standard techniques[50]. After castration at 8 weeks of age, mice were allowed to regress for 4 weeks to reach the fully involuted state. For tamoxifen induction of Cre activity in mice containing the *Nkx3-1*^{CreERT2} allele, mice were administered 9 mg per 40 g tamoxifen (Sigma) suspended in corn oil, or vehicle alone for negative controls, by intraperitoneal injection or oral gavage once daily for 4 consecutive days, followed by a chase period of 14 days.

For prostate regeneration, testosterone (Sigma) was dissolved at 25 mg ml^{-1} in 100% ethanol and diluted in PEG-400 to a final concentration of 7.5 mg ml^{-1}. Testosterone was administered for 4 weeks at a rate of 1.875 μg h^{-1} delivered by subcutaneous implantation of mini-osmotic pumps (Alzet); this regimen yields physiological levels of serum testosterone[45]. When included, BrdU (100 mg kg^{-1}) (Sigma) was also administered by intraperitoneal injection once daily during the first 3 days of regeneration to label proliferating cells. After regeneration of the prostate, mice could be euthanized for analysis, or deprived of androgens by pump removal, returning to the regressed state after 4 more weeks. At this point, mice were either euthanized for analysis, or osmotic pumps could be reimplanted for further rounds of serial regression/regeneration.

For tissue recombination and renal grafting, prostate tissues (corresponding to the combined anterior, dorsolateral and ventral lobes) were dissected and minced to small clumps, followed by enzymatic dissociation with 0.2% collagenase I (Invitrogen) in DMEM media with 10% FBS for 90 min. Dissociated tissue was passed sequentially through 21-, 23- and 26-gauge needles followed by a 40-μm cell strainer to obtain single-cell suspensions. The resulting cells were assessed for viability by trypan blue exclusion and counted. For grafts containing large numbers of epithelial cells, as in Supplementary Fig. 4, 2.5×10^5 dissociated prostate cells obtained from castrated and tamoxifen-induced *Nkx3-1*$^{CreERT2/+}$; *R26R-YFP/+* mice were mixed with 2.5×10^5 dissociated urogenital sinus mesenchyme (UGM) cells from embryonic day (E) 18.0 rat embryos. UGM cells were obtained from dissected urogenital sinus that was treated for 30 min in 1% trypsin, followed by mechanical dissociation and treatment with 0.1% collagenase B (Roche) for 30 min at 37 °C, and washing in PBS. Pelleted cell mixtures were resuspended in 10 μl of 1:5 collagen:setting buffer (10× Earle's Balanced Salt Solution (Life Technologies), 0.2 M $NaHCO_3$ and 50 mM NaOH), and gelatinized in 37 °C for 20 min. Tissue recombinants were cultured in DMEM media with 10% FBS supplemented with 10^{-7} M dihydrotestosterone (DHT) overnight, followed by transplantation under the kidney capsules of *nude* mice. Grafts were collected after 4–8 weeks of growth for analysis.

For single-cell grafts, as in Fig. 3, a single YFP$^+$ (or YFP$^-$ cell as a control) was isolated from the dissociated cell suspension from castrated and tamoxifen-induced *Nkx3-1*$^{CreERT2/+}$; *R26R-YFP/+* prostates by mouth-pipetting under epifluorescence illumination on an Olympus IX51 inverted microscope with DP71 camera. This single cell was then recombined with 2.5×10^5 dissociated UGM cells obtained from E18.0 rat embryos, and cultured and grafted as above. Grafts were collected after 10–12 weeks of growth for analysis, and imaged under epifluorescence on an Olympus SZX16 stereomicroscope with DP71 camera. The resulting graft tissue was analysed for YFP and other marker expression as described later, and counterstained with DAPI for visualization of nuclear morphology at high-power to distinguish mouse from rat nuclei[31].

Grafts recovered from transplantation of a single lineage-marked YFP$^+$ cell ($n = 16$ out of 43, 37%) were confirmed to be of mouse origin by YFP expression and nuclear morphology (Supplementary Fig. 6), whereas the single graft ($n = 1$ out of 31, 3%) arising from a YFP$^-$ cell was confirmed to be of mouse origin by nuclear morphology. Generation of prostatic ducts by a YFP$^-$ cell might result from a CARN that was not lineage-marked by tamoxifen-induction, which is inefficient, or alternatively from a distinct stem cell type in the prostate epithelium. We note that a considerable percentage ($n = 13$ out of 74, 18%) of the grafts contained ducts of rat origin, which are not included in Fig. 3j. These rat ducts probably arise from rat urogenital epithelial cells that are difficult to completely dissociate from the urogenital mesenchyme used in the graft, and can populate the graft under conditions in which the epithelial contribution is limiting.

For histological and immunofluorescence analysis, individual prostate lobes or renal grafts were dissected, and then fixed in 4% paraformaldehyde for subsequent cryoembedding in OCT compound (Sakura), or fixed in 10% formalin followed by paraffin embedding. The volume of dissected anterior prostate lobes was determined by physical displacement of known volumes of PBS solution in 0.5-ml centrifuge tubes.

Histology and immunostaining. H&E staining was performed using standard protocols on 6-μm paraffin sections. β-galactosidase staining was performed using 12-μm cryosections, which were incubated in staining solution (0.1 M PBS, 1.3 mM $MgCl_2$, 1 mg ml^{-1} X-gal, 0.02% Nonidet P–40, 5 mM $K_4Fe(CN)_6$, 5 mM $K_3Fe(CN)_6$ and 0.01% Na-deoxycholate) for 3 h or overnight, followed by fixation in 10% formalin for 2–5 h. Direct visualization of YFP was performed after washing 10-μm cryosections in PBST (PBS with 0.1% Triton X-100) three times, incubation with TOPRO3 (1:1,000 diluted in PBST) (Invitrogen/Molecular Probes) for 30 min, and mounting with VECTASHIELD mounting medium (Vector Labs), which contains DAPI.

For immunohistochemical staining, 6-μm paraffin sections were deparaffinized in xylene, followed by antigen retrieval through boiling in antigen unmasking solution (Vector Labs). Slides were blocked in 10% normal serum or with blocking reagents provided in the M.O.M. ('Mouse-on-Mouse') immunodetection kit (Vector Labs) for mouse primary antibodies, then incubated with primary antibodies overnight at 4 °C or room temperature. Primary antibodies and dilutions used are listed in Supplementary Table 5. Secondary antibodies were obtained from Vectastain ABC kits (Vector Labs) and diluted 1:250 or 1:500. The signal was enhanced using the Vectastain ABC system and visualized with the NovaRed Substrate Kit (Vector Labs). The slides were counterstained with Harris Modified Hematoxylin (diluted 1:4 in H_2O) (Fisher Scientific) and mounted with Clearmount (American Master*Tech Scientific). Immunohistochemical staining was imaged using a Nikon Eclipse E800 microscope equipped with a Nikon DXM1200 digital camera.

Immunofluorescence staining was performed on either 6-μm paraffin sections or 10-μm cryosections, which were incubated in 3% H_2O_2 and Antigen Unmasking Solution (Vector Labs). Primary antibodies and dilutions used are listed in Supplementary Table 5. Slides were incubated with 10% normal goat serum (Vector Labs) or donkey serum (Sigma) and with primary antibodies diluted in the 10% normal goat or donkey serum overnight at 4 °C or room temperature. Slides then were incubated with secondary antibodies (diluted 1:500 in PBST) labelled with Alexa Fluor 488, 555, or 594 (Invitrogen/Molecular Probes). Detection of Nkx3-1, green fluorescent protein (GFP) and Cre was enhanced using tyramide amplification (Invitrogen/Molecular Probes) by incubation of slides with horseradish peroxidase (HRP)-conjugated secondary antibody (1:100 dilution) (Invitrogen/Molecular Probes), followed by incubation with tyramide 488 or 555 for 6min. Sections were counterstained with TOPRO3 or TOTO3 (diluted 1:1,000 in PBST) (Invitrogen/Molecular Probes) to visualize nuclei, and mounted with VECTASHIELD mounting medium (Vector Labs),

which contains DAPI. Immunofluorescence staining was imaged using a Leica TCS5 spectral confocal microscope.

Quantification and statistics. To calculate the number of CARNs in the regressed mouse prostate, we determined that there are an average of 112,000 total cells ($n = 5$ animals; all lobes combined), of which 59% are epithelial as determined by immunoreactivity for the pan-epithelial marker CD24 (ref. 9). Because 0.7% of epithelial cells in the regressed prostate are CARNs, there are approximately 460 CARNs in the total prostate. To determine the number of lineage-marked cells in the regressed prostate, we visualized 320 live YFP^+ cells in dissociated prostate tissue (all lobes combined) from five castrated lineage-marked *Nkx3-1*$^{CreERT2/+}$*; R26R-YFP/+* mice, for a total of 64 YFP^+ live cells/mouse. For the experiment in Supplementary Fig. 4, we performed two recombinations from these dissociated prostate cells, so that there were approximately 160 live YFP^+ cells used in each graft.

For immunostaining experiments, cell numbers were counted manually using confocal ×40 and ×63 photomicrographs. Statistical analyses were performed using a two-sample *t*-test, χ^2 test, or Fisher's Exact test as appropriate. At least three animals for each experiment or genotype were analysed.

46. Nagy, A., Gertsenstein, M., Vintersten, K. & Behringer, R. *Manipulating the Mouse Embryo: A Laboratory Manual* Chs 8–11 359–506 (Cold Spring Harbor Laboratory Press, 2003).
47. Bunting, M., Bernstein, K. E., Greer, J. M., Capecchi, M. R. & Thomas, K. R. Targeting genes for self-excision in the germ line. *Genes Dev.* **13,** 1524–1528 (1999).
48. Tybulewicz, V. L., Crawford, C. E., Jackson, P. K., Bronson, R. T. & Mulligan, R. C. Neonatal lethality and lymphopenia in mice with a homozygous disruption of the *c-abl* proto-oncogene. *Cell* **65,** 1153–1163 (1991).
49. Deng, C., Wynshaw-Boris, A., Zhou, F., Kuo, A. & Leder, P. Fibroblast growth factor receptor 3 is a negative regulator of bone growth. *Cell* **84,** 911–921 (1996).
50. Gao, H., Ouyang, X., Banach-Petrosky, W. A., Shen, M. M. & Abate-Shen, C. Emergence of androgen independence at early stages of prostate cancer progression in *Nkx3.1; Pten* mice. *Cancer Res.* **66,** 7929–7933 (2006).